Title

The role of adhesion junctions in the biomechanical behaviour and osteogenic differentiation of 3D mesenchymal stem cell spheroids

Authors

Griffin, FE
Schiavi, J
McDevitt, TC
et al.

Publication Date

2017-07-01

DOI

10.1016/j.jbiomech.2017.05.014

Peer reviewed

HHS Public Access

Author manuscript

J Biomech. Author manuscript; available in PMC 2019 February 27.

Published in final edited form as:

J Biomech. 2017 July 05; 59: 71–79. doi:10.1016/j.jbiomech.2017.05.014.

The role of adhesion junctions in the biomechanical behaviour and osteogenic differentiation of 3D mesenchymal stem cell spheroids

F.E. Griffin[a], **J. Schiavi**[a], **T.C. McDevitt**[b], **J.P. McGarry**[a], and **L.M. McNamara**[a,*]

[a]Biomechanics Research Centre (BMEC), Biomedical Engineering, College of Engineering and Informatics, National University of Ireland, Galway, Ireland [b]Gladstone Institute, University of California, San Francisco, USA

Abstract

Osteogenesis of mesenchymal stem cells (MSC) can be regulated by the mechanical environment. MSCs grown in 3D spheroids (mesenspheres) have preserved multi-lineage potential, improved differentiation efficiency, and exhibit enhanced osteogenic gene expression and matrix composition in comparison to MSCs grown in 2D culture. Within 3D mesenspheres, mechanical cues are primarily in the form of cell-cell contraction, mediated by adhesion junctions, and as such adhesion junctions are likely to play an important role in the osteogenic differentiation of mesenspheres. However the precise role of N-and OB-cadherin on the biomechanical behaviour of mesenspheres remains unknown. Here we have mechanically tested mesenspheres cultured in suspension using parallel plate compression to assess the influence of N-cadherin and OB-cadherin adhesion junctions on the viscoelastic properties of the mesenspheres during osteogenesis. Our results demonstrate that N-cadherin and OB-cadherin have different effects on mesensphere viscoelastic behaviour and osteogenesis. When OB-cadherin was silenced, the viscosity, initial and long term Young's moduli and actin stress fibre formation of the mesenspheres increased in comparison to N-cadherin silenced mesenspheres and mesenspheres treated with a scrambled siRNA (Scram) at day 2. Additionally, the increased viscoelastic material properties correlate with evidence of calcification at an earlier time point (day 7) of OB-cadherin silenced mesenspheres but not Scram. Interestingly, both N-cadherin and OB-cadherin silenced mesenspheres had higher BSP2 expression than Scram at day 14. Taken together, these results indicate that N-cadherin and OB-cadherin both influence mesensphere biomechanics and osteogenesis, but play different roles.

Keywords

Cadherin; Mesenchymal stem cell; Suspension culture; Biomechanics; Viscoelastic

*Corresponding author. laoise.mcnamara@nuigalway.ie (L.M. McNamara).

Authors' contributions

FEG, TCM, JPM and LMM conceived and designed the experiments. FEG and JS performed the experiments and data analysis. All authors contributed to data interpretation, manuscript preparation and editing. All authors read and approved the final manuscript.

Conflict of interest

All authors declare no financial or competing interests.

1. Introduction

Mesenchymal stem cells (MSCs) have emerged as an attractive cell source for osteogenic tissue engineering and regenerative medicine treatments for bone defects resulting from disease or trauma. The exploitation of MSCs for treatment of bone disease requires further study of regulating factors, such as the biochemical and mechanical environment, which influence the osteogenic differentiation of MSCs. In vitro, MSCs are commonly cultured in monolayers or on biomaterial scaffolds for the purposes of large scale expansion, to study their biology and investigate how they respond to extracellular biochemical and mechanical stimulation (Simmons et al., 2003; Luu et al., 2007; Mani et al., 2008; Wang et al., 2010; Fujita et al., 2014). Both of these culture methods rely on cell-substrate interactions, which strongly influence the biology and mechanics of the MSCs (Engler et al., 2006; Huebsch et al., 2010). Suspension culture approaches, such as scaffold-free MSC spheroids (mesenspheres) (Wang et al., 2009; Baraniak and McDevitt, 2012; Cook et al., 2012; Kabiri et al., 2012) offer an environment dominated by the biophysical behaviour of the cells rather than extracellular substrates. These studies have demonstrated that MSCs grown in mesenspheres have preserved multi-lineage potential (Baraniak and McDevitt, 2012), improved differentiation efficiency (Wang et al., 2009), and exhibit enhanced osteogenic gene expression and matrix composition in comparison to MSCs grown in 2D culture (Kabiri et al., 2012).

Stem cell differentiation in vivo is strongly regulated by both intrinsic and extrinsic signalling within the stem cell microenvironment, including cell-cell interactions, factors secreted by cells, and cellular interactions with extracellular structures (Watt and Hogan, 2000; Yin and Li, 2006). During intramembranous ossification, one of the two essential processes by which bone is formed during fetal development, MSCs condense into areas of closely contacting cells (Thompson et al., 1989). These MSCs are connected via transmembrane adhesion junctions, comprised of extracellular glycoproteins known as cadherins, which facilitate cell-cell adhesion (Oberlender and Tuan, 1994). Cadherins form a connection between the cytoskeleton of adjacent cells by bonding with cadherins on neighbouring cells (Overduin et al., 1995; Shapiro et al., 1995; Stains and Civitelli, 2005). The condensed cell aggregates then begin to differentiate, form a membrane known as the periosteum and begin to produce a rudimentary bone matrix within this membrane (Gilbert, 2000; Hall and Miyake, 2000; Karaplis, 2002; Kanczler and Oreffo, 2008). In light of the close-contact established during MSC condensation, which initiates intramembranous ossification, mesenspheres offer a comparable environment to elicit osteogenic differentiation of MSCs along the intramembranous pathway.

The mechanical behaviour of MSCs is dictated by the cytoskeleton and is significantly influenced by cytoskeletal realignment and stress fibre formation (Titushkin and Cho, 2007). Adhesion junctions are mechanosensitive structures that play an important role in the biomechanical behaviour of cells due to their involvement in the transmission of forces generated by the cytoskeleton (Ganz et al., 2006; Ladoux et al., 2010; Yonemura et al., 2010; Chopra et al., 2011; Maruthamuthu et al., 2011; Huveneers et al., 2012). Adhesion junctions also regulate the expression of osteogenic transcription factors in a manner related to the

mechanical environment of the cells (Nelson and Nusse, 2004; Guntur et al., 2012). However the mechanisms by which MSCs, cultured as 3D mesenspheres, sense and respond to their environment are still unclear as investigations into cell mechanosensation have typically been carried out in 2D culture systems (Ladoux et al., 2010; Chopra et al., 2011; Maruthamuthu et al., 2011).

N-cadherin and OB-cadherin are the main cadherins expressed by MSCs and osteoblasts (Kawaguchi et al., 2001; Hsu and Huang, 2013). N-cadherin expression decreases with osteogenic differentiation of MSCs whereas OB-cadherin expression increases (Kawaguchi et al., 2001; Hsu and Huang, 2013). During in vitro culture, the expression level of N-cadherin increases in MSCs grown in 3D spheroids in comparison to those grown in 2D (Hsu and Huang, 2013). The extracellular mechanical environment and exogenous stimulation can induce a phenotypic shift towards osteogenic differentiation (Engler et al., 2004; Mullen et al., 2013; Tan et al., 2014). Within 3D spheroids, mechanical cues are primarily in the form of cell-cell contraction, mediated by adhesion junctions, and as such adhesion junctions are likely to play an important role in the osteogenic differentiation of mesenspheres. However the precise role of N- and OB-cadherin on the biomechanical behaviour of mesenspheres remains unknown.

This study tested the hypothesis that adhesion junctions play an important role in dictating the mesensphere mechanical environment. The primary objective was to investigate the influence of N-cadherin and OB-cadherin adhesion junctions and stress fibre formation in the mechanical behaviour of mesenspheres during osteogenesis. The suspension culture system used provides a useful method to investigate cadherin mechanobiology in the absence of the confounding factor of cell-substrate interaction. This investigation was carried out by silencing N-cadherin or OB-cadherin adhesion junctions with siRNA and measuring mesensphere viscoelastic properties. Additionally we examined changes in cell morphology and osteogenic differentiation of the mesenspheres to ascertain the role of N-cadherin, OB-cadherin and the cytoskeleton on mesensphere biomechanics.

2. Methods

2.1. Mesensphere formation and culture

C57BL/6 mouse mesenchymal stem cell (MSC) monolayers (CliniSciences) were expanded in MSC expansion media (IMDM (Gibco) supplemented with 10% fetal bovine serum (Hyclone), 10% horse serum (Hyclone) and 2 mM L-glutamine (Corning)). Cells were maintained in a humidified incubator at 37 °C and 5 % CO_2. MSCs were dissociated from adherent culture with 0.25% Trypsin (Corning). MSC spheroids (Mesenspheres) were formed using a forced aggregation technique (Zimmermann and McDevitt, 2014) whereby cells are centrifuged (200 rcf) into 400 μm diameter 3% agarose (Fisher) microwells (Aggrewell™ StemCell Technologies INC). MSCs were seeded (3×10^6) into 6000 microwells, yielding mesenspheres of approximately 500 cells (Fig. 1A). After 12 h of spheroid formation in microwells, mesenspheres were transferred to 100 mm bacteriological grade petri dishes (approximately 1500 mesenspheres per petri dish) and cultured in suspension in 10 mL osteogenic supplemented media (MSC expansion media without FBS, supplemented with 100 nM Dexamethasone, 50 μg/ml Ascorbic Acid, 10 mM β-glycerol

Phosphate (all Sigma)) on a rotary orbital shaker platform at 65 rpm, similar to previously described methods for culture of embryonic stem cell spheroids (Kinney et al., 2012). Media was exchanged every 3–4 days.

2.2. siRNA treatment

The small interfering RNA (siRNA) oligonucleotides for N-cadherin (sc-35999), OB-cadherin (sc-36114) and a scrambled control (sc-37007) were obtained from Santa Cruz. MSC monolayers at 80–90% confluency in 150 mm bacteriological petri dishes were washed three times with 10 mL Phosphate Buffered Saline (PBS) solution and then treated with 80 nM siRNA and 128 μL Lipofectamine 2000 (Invitrogen) in 8 mL of Opti-MEM (Gibco) for 20 h prior to mesensphere formation. Knockdown efficiency of siRNA for cadherin protein expression was assessed by Western Blot and compared to untreated cells and cells treated with non-specific scrambled siRNA (Fig. 1B and C).

2.3. Western blot

Mesenspheres were lysed using CelLytic™ M cell lysis reagent (Sigma) for 15 min at room temperature and then centrifuged (12,000 g) for 15 min to pellet cell debris. Supernatant was transferred to chilled microcentrifuge tubes and stored at −20 °C. A Coomassie Plus protein assay (Thermo Scientific) was performed to quantify total protein. 50 μg of protein was diluted with 20% 5X loading buffer (1.25 mL 0.5 M Tris-HCl, pH 6.8, 1 g SDS (Fisher), 5 mL glycerol (VWR), 5 mg Bromophenol Blue (Sigma), 1.25 mL βME (Sigma), deionised water) and heated to 95 °C for 5 min. Cell lysates were run on 12 % Mini-PROTEAN®TGX™ gels (Bio-Rad) with 5 μL SeeBlue® Plus2 Prestain (Invitrogen), blotted, and proteins were probed with 1:1000 N-cadherin (sc-7939, Santa Cruz) or 1:1000 OB-cadherin (ab151302, Abcam) primary antibody, and a horseradish peroxide (HRP) conjugated secondary antibody (1:1000) (Santa Cruz) and then detected by chemiluminescent (ECL) substrate. Knockdown of cadherins was quantified using Image Studio Lite software from LI-COR Biosciences.

2.4. Mesensphere mechanical testing methods

A parallel plate testing system (Microsquisher, CellScale) was used to measure the micro-scale mechanical properties of mesenspheres from non-siRNA treated (control) groups and N-cadherin (—N), OB-cadherin (—OB) and a scrambled control (Scram) siRNA treatment groups at days 2, 7 and 14. This system calculates force via the measurement of beam deflection in response to user defined displacements. All samples were tested in a PBS (Corning) fluid bath. Mesenspheres were loaded onto a glass platform and compressed by cantilever beams made of Tungsten (Young's Modulus = 411 GPa). The diameter of the cantilever beams varied from 152.4 μm to 304.8 μm, depending on the relative stiffness of the mesenspheres.

Creep tests were performed to determine the viscoelastic properties of mesen-spheres, with the time dependent deformation of the sample being measured under a constant applied force (Fig. 2). The magnitude of force for the creep test was chosen as the average force corresponding to approximately 40% decrease in mesensphere height. This was determined based on constant strain rate analysis of stress versus vertical strain in $n = 6$ samples for each

time point and condition before commencing creep testing. Steady state deformed configuration is identified from creep test results (Kinney et al., 2014. A minimum of 19 distinct, randomly chosen mesenspheres were creep tested for each time point and condition. The mesensphere is assumed to behave as a homogeneous, isotropic, incompressible standard linear solid viscoelastic material. The nominal axial creep strain at time t, is given as $\varepsilon(t) = u(t)/H_0$, where $u(t)$ is the change in height of the mesensphere and H_0, the initial undeformed mesensphere height (diameter). σ_0 is the applied stress, and was normalised to D_0, the initial mesensphere horizontal diameter. The instantaneous modulus, E_o, the long term modulus, E_∞, and viscosity, μ, are determined by fitting (Eq. 1) to experimental creep curves.

$$\varepsilon(t) = \frac{2\sigma_0}{3E_\infty}\left[1 + \left(\frac{E_\infty}{E_0} - 1\right)\exp\left(-tE_\infty\left(E_0 - E_\infty\right)/\mu E_0\right)\right] \quad (1)$$

2.5. Histological and immunofluorescent staining

4% paraformaldehyde was used to fix mesenspheres at room temperature for 30 min. Mesenspheres were rinsed with PBS, embedded within Histogel (Thermo Scientific), and then processed through a series of ethanol and xylene rinses before paraffin embedding. Mesenspheres embedded within paraffin were sectioned at a thickness of 10 μm and then mounted on SuperFrost Plus slides (Fisher). Prior to staining, mesensphere sections were deparaffinised using a series of ethanol and xylene rinses. Histological staining was done using Gills' III Modified Hemotoxylin and 1% Eosin Y, Alcoholic Solution (Harleco) to observe cells repartition. For mineralisation, 2% Alizarin Red solution was added to sections (all Sigma) (Freeman et al., 2013, 2015, 2016) (Freeman et al., 2013, 2015, 2016). After the staining, the samples were dehydrated through a series of increasing concentration of ethanol, rinsed with xylene rinses, and mounted with DPX. For fluorescent staining, cell membranes were first permeabilised and blocked using a solution of 0.1% Triton™ X-100 (Sigma) and 1% Donkey serum or Bovine Serum Albumin (Sigma) in PBS for 1 h. For observing the cytoskeleton, samples were incubated 1:1000 Phalloidin TRITC (P1951, Sigma) and Fluoroshield mounting media with DAPI (F6057, Sigma). For the immunofluorescent staining of the Bone Sialoprotein 2 (BSP2), the primary antibody was added overnight at 4 °C on samples (dilute 1:100 in PBS, Santa Cruz). After 3 washes with PBS, the secondary antibody was added during 1 h at room temperature on samples (1:200 in PBS, JacksonImmunoResearch) and washed three timesbefore mounting on a slide using mounting media.

2.6. Immunofluorescent Image analysis

ImageJ software (Fiji) was used to quantify the variation in the actin cytoskeleton between treatment groups ($n = 6$ aggregates per group). The raw Phalloidin TRITC channel was thresholded to remove nonspecific background staining. The percentage of the mesensphere cross-sectional area that was above the threshold was recorded. The corrected total cell fluorescence per area surface of BSP2 were measured using ImageJ (v 1.49, NIH) as it was

done (McCloy et al., 2014) by calculating (Integrated Density – (Area selected X Mean fluorescence of background readings))/area surface.

2.7. Statistical analysis

For creep testing results, statistics were performed using Minitab on $n = 19$ individual mesenspheres for each group. Statistical tests between treatment group and time point were carried out using Kruskal-Wallis non-parametric test between individual groups when data was non-normally distributed or had unequal variance. A Levene's test for equal variance was conducted on each group to test for variance. Statistical significance was declared at $p \leq 0.05$. To analyse the correlation between mesensphere diameter and viscosity or Young's moduli, a Pearson's Correlation coefficient (r) for each treatment group and time point was calculated. r ranges from −1 for a perfect negative linear relationship to +1 for a perfect positive linear relationship between two variables. Correlation was considered significant if $r \leq -0.6$ or $r \geq 0.6$ and if $p \leq 0.05$. The band in each box plot represents the data median, and the cross represents the mean. Boxplot whiskers extend to data points that are less than 1.5 × Interquartile Range from the 1st/3rd quartile.

3. Results

3.1. Osteogenic differentiation increases mesensphere viscosity and long term Young's modulus

The viscosity (μ), instantaneous Young's modulus (E_0) and long term Young's modulus (E_∞) of non-siRNA treated mesenspheres (Cont) increased with osteogenic differentiation between days 2, 7 and 14 (Fig. 3). This was demonstrated by significantly increased viscous resistance to deformation at day 14 in comparison to day 2 and day 7 ($p < 0.001$). A significant increase in E_∞ at day 14 in comparison to days 2 and 7 ($p < 0.001$) was observed (Fig. 3). A significant increase in E_0 at day 14 in comparison to days 2 and 7 ($p < 0.001$) was also observed (Fig. 3). Osteogenesis of Control mesenspheres was evident by the increased calcium deposition between day 7 and day 14 (Fig. 6). BSP-2 staining did not increase between days 7 and 14.

3.2. Scrambled siRNA treatment decreases mesensphere viscosity and long term Young's modulus

The scrambled siRNA treated mesenspheres (Scram) stained positively for calcification (Fig. 6) and had significantly higher μ, E_0 and E_∞ than Control at day 7 ($p = 0.006$, $p = 0.016$, $p = 0.006$ respectively). The Control mesenspheres did not stain positively for calcification at Day 7. By Day 14, scrambled siRNA treated mesenspheres (Scram) had significantly lower μ and E_∞ ($p = 0.001$, $p < 0.001$ respectively) and less homogenous calcification than Cont mesenspheres (Figs. 3 and 6). Together, these results indicate a significant effect of siRNA treatment on the mesensphere viscoelastic behaviour and osteogenic differentiation. Mean and standard deviation values of μ, E_0 and E_∞ are detailed in Table 1.

3.3. OB-cadherin siRNA treatment increases mesensphere viscosity, long term Young's modulus and early calcification

The effects of the siRNA silencing of N-cadherin (—N) and OB-cadherin (—OB) on mesensphere μ, E_0 and E_∞ were most apparent at day 2. At day 2 the μ, E_0 and E_∞ (Fig. 4) of —OB mesenspheres were significantly increased in comparison to scrambled ($p < 0.001$, $p < 0.001$, $p < 0.001$ respectively) and —N mesenspheres ($p < 0.001$, $p < 0.001$, $p < 0.01$ respectively). —N showed significantly lower μ, E_0 and E_∞ than scrambled and —OB mesenspheres at day 7 ($p < 0.012$, $p < 0.01$, $p < 0.002$ respectively). At day 7, localised areas of calcification can be seen in —OB mesenspheres but not in other groups (Fig. 6). Furthermore —OB and —N groups exhibited areas of strong BSP-2 staining at day 7 and 14 whereas the Scram group did not (Fig. 7). By day 14, there was no significant difference between μ, E_0 and E_∞ for Scram, —N and —OB mesenspheres and each had some non-homogenous mesensphere calcification.

Mesenspheres from all groups displayed a significant increase in μ (all $p < 0.001$), E_0 (all $p < 0.001$) and E_∞ (all $p < 0.004$) between days 2 and 14 (Figs. 3 and 4). Scram, —N and —OB demonstrated more calcification and BSP-2 staining at day 14 than day 7. —OB had calcification nodules at day 7 and by Day 14 there was a more even distribution of calcification.

3.4. OB-cadherin silencing increases stress fibre formation

Silencing of OB-cadherin resulted in a significant increase in the cytoskeletal network of mesenspheres in comparison to scrambled (—OB vs. Scram, day 2: $p < 0.0001$, day 7: $p = 0.003$) and —N (—OB vs. —N, day 2: $p = 0.017$, day 14: $p = 0.020$) mesenspheres (Fig. 5A and C). At all time-points, —N stress fibre formation did not significantly differ from Scram. This indicates that OB-cadherin may have more influence on stress fibre formation than N-cadherin adhesion junctions. H & E staining demonstrated no discernible difference in cellular morphology between mesenspheres of different groups or time points at days 2, 7 or 14 (Fig. 5B).

3.5. Mesensphere size effects of siRNA treatment

Treatment of MSCs with siRNA resulted in a larger maximum diameter (D_0) of —N mesenspheres ($D_0 = 380$ μm) than —OB ($D_0 = 223$ μm) and Scram ($D_0 = 259$ μm) at day 2 (Fig. 5D). Larger —N mesenspheres could be indicative of impaired initial compaction of the cells, suggesting a role for N-cadherin in initial mesensphere formation. At days 2, 7 and 14, there was a strong negative correlation between mesensphere horizontal diameter and μ, E_0 or E_∞ for Scram mesenspheres (Table 2), i.e., larger mesenspheres showed less viscous resistance to deformation. —OB mesenspheres had a significant negative correlation at day 2 for μ and E_∞ and day 7 E_0 and E_∞, Untreated mesenspheres had a negative correlation between horizontal diameter and μ, E_0 or E_∞ at day 7. —N mesenspheres displayed a positive correlation between horizontal diameter and μ but a negative correlation with μ, E_0 or E_∞ at day 14.

4. Discussion

The overall goal of this study was to investigate the role of adhesion junctions and cytoskeleton stress fibre formation in the mechanical behaviour of mesenspheres undergoing osteogenic differentiation. Mesensphere mechanical behaviour and morphology were analysed at days 2, 7 and 14 to investigate the contribution of N-cadherin or OB-cadherin adhesion junctions and the cytoskeleton to the mechanics of the mesensphere. It was found that silencing of N-cadherin (—N) or OB-cadherin (—OB) expression yielded different effects on the mesenspheres. When OB-cadherin was silenced, the viscosity (μ), initial Young's modulus (E_0), long term Young's modulus (E_∞) and actin stress fibre formation of the mesenspheres increased in comparison to —N mesenspheres and mesenspheres treated with a scrambled siRNA (Scram) at day 2. At day 7 —OB had significantly higher μ, E_0, E_∞ than —N or Scram mesenspheres. Moreover the —OB group had more intense calcification, in the form of large nodules, than the —N or Scram mesenspheres. By day 14 —OB had significantly higher E_∞, and calcification was more evenly distributed across the mesensphere than Scram. By Day 14 the —N and —OB mesenspheres had higher BSP2 production than Scram, but —N had less mineral than all other groups. Taken together, these results indicate that N-cadherin and OB-cadherin both influence mesensphere biomechanics and osteogenesis, but play different roles.

A potential limitation of this study is the compacted arrangement of cells in a mesensphere, which might lead to diffusion difficulties for nutrients and molecules through 3D constructs due the size of the construct (Sachlos and Auguste, 2008). However, mesenspheres of 300, 600 or 1000 cells grown in a similar orbital suspension system did not exhibit evidence of necrotic core formation through 14 days of culture and <5% of the cells in the mesensphere had BrdU staining to indicate proliferation was occurring (Baraniak and McDevitt, 2012). Secondly, the results presented here demonstrate that mesenspheres treated with scrambled siRNA had a higher μ, E_0 and E_∞ than untreated cells at day 7, and lower at day 14. However, previous work using a scrambled siRNA on fibroblasts demonstrated a lower Young's modulus than control cells (Lee et al., 2012). In the work presented here mesenspheres treated with N-cadherin or OB-cadherin siRNA were compared to those treated with scrambled siRNA, rather than untreated cells, so as to account for any change in μ, E_0 and E_∞ resulting from siRNA treatment alone. siRNA transfection using lipofectamine is a possible limitation of this study, as the long term knock-down of N-cadherin or OB-cadherin is not confirmed. Long term, siRNA treatment resulted in significantly lower μ, E_0 and E_∞ for Scram in comparison to Cont at day 14, but this could be in part due to less homogenous calcification of the mesensphere (Fig. 6). Control mesenspheres were calcified throughout, whereas Scram mesenspheres were strongly calcified only in part of the mesensphere. However, early inhibition of N-cadherin and OB-cadherin was confirmed, and did effect the osteogenesis of mesenspheres at later time points (Figs. 6 and 7). The assumption of small deformations used in the Standard Linear Solid (SLS) material model used to calculate the material properties of the mesenspheres creates a possible limitation. Mesenspheres experienced strains up to approximately 70%. However, previous studies have demonstrated that the infinitesimal strain assumption may still be accurate for a viscoelastic halfspace model under micropipette aspiration (cellular strains of greater than 30% were

generated) (Haider and Guilak, 2002). The parallel plate compression testing system used here is advantageous as it allows for the measurement of the creep strain of a composite material consisting of >500 cells. In comparison, testing of single cells (e.g. Atomic Force Microscopy (AFM)) will result in a high level of variability between samples, and the assumption of a homogeneous isotropic material cannot be justified when choosing a model to interpret single cell data (Reynolds and McGarry, 2015; Weafer et al., 2015).

Creep testing of spherical aggregates of embryonic stem cells (EBs) has been performed using the same parallel plate compression testing system (Kinney et al., 2014). The long term Young's modulus of EBs was 0.21 kPa after 14 days of mesenchymal differentiation (Kinney et al., 2014). The results presented in the current paper for control mesenspheres at day 2 reveal that the E_∞ (1.58 ± 0.31 kPa) is approximately threefold higher than the E_∞ for spherical, unspread MSCs (0.47 ± 0.52 kPa) as measured using AFM testing of single cells (Darling et al., 2008). Interestingly, the control mesensphere E_∞ was approximately 0.7 that of spread MSCs (2.27 ± 1.9 kPa). In contrast to unspread cells, spread cells exhibit highly developed stress fibres. A previous study by (Ronan et al., 2012) demonstrates that the contractile stress fibre network significantly increases the compression resistance of the cell. While cells in mesenspheres do not exhibit the extensive stress fibre network reported for cells spread on stiff substrates, mesenspheres do possess some stress fibres due to the mechanical stimulus generated between neighbouring cells that is transmitted via cell-cell adhesions. Additionally, increased μ, E_0 and E_∞ at day 14 vs day 2 for all groups correlates with calcification of the mesenspheres between day 7 and 14 and increase BSP-2 for —N and —OB mesenspheres. At day 7 —OB has significantly higher μ, E_0 and E_∞ than —N which is likely due to early calcification of —OB, indicated by the dark nodules of calcification seen at this time-point.

Previous work has shown that the elastic modulus of MSCs is significantly influenced by the cytoskeleton (Titushkin and Cho, 2007). Adhesion junctions transmit mechanical forces such as cytoskeletal tension between cells (Ganz et al., 2006; Maruthamuthu et al., 2011) and are strengthened and stabilised by interaction with the cytoskeleton (Pittet et al., 2008; Liu et al., 2010; Hong et al., 2013; Ronan et al., 2015). In this study we demonstrate that the cytoskeleton/adhesion junction relationship is reciprocal; adhesion junctions also influence stress fibre formation and mesensphere mechanical behaviour. Specifically, we observed for the first time that increases in stress fibre formation, μ, E_0 and E_∞ occur when OB-cadherin expression is decreased in mesenspheres. Interestingly, the increase in μ, E_0 and E_∞ between days 2 and 7 for Scram mesenspheres does not coincide with an increase in stress fibre formation. The gradual increase in μ, E_0 and E_∞ from Day 2 to Day 14 for mesenspheres within each treatment group is likely due to the osteogenic differentiation of the mesenspheres (Figs. 6 and 7). Scram and —OB mesenspheres showed a trend of decreasing stress fibre formation between days 2 and 7, but a significant increase only occurred between days 7 and 14 coinciding with increased calcium staining for Scram, and more homogeneous calcium staining of —OB. —N mesenspheres had no significant difference in stress fibre formation between time points but had increased BSP2 expression between days 7 and 14. Previous studies have shown that N-cadherin and OB-cadherin expression increase with osteogenic differentiation (Shin et al., 2000) and the work presented here explores the different functions of these cadherins during osteogenesis. The results of this study indicate

that —OB mesenspheres have increased viscoelastic material properties and deposit calcium earlier than Scram mesenspheres, while —N mesenspheres have similar viscoelastic material properties to Scram but elevated BSP2 production at later time points. The different influences on stress fibre formation, μ, E_0 and E_∞ and osteogenesis indicate that N-cadherin plays different role in MSC regulatory mechanisms for osteogenesis and cell mechanical properties than OB-cadherin.

Acknowledgements

We thank Christian Mandrycky and Janna Luessing for their invaluable help with western blotting. We also thank Joshua Zimmermann and Melissa Kinney for their time and expertise with regards to the suspension culture and mechanical testing methods. The authors would like to thank the students and staff of the Wallace H. Coulter Department of Biomedical Engineering at Georgia Institute of Technology were this work was carried out.

Funding

This work was supported by the BMERM Structured PhD programme funded by the European Regional Development Fund, the Higher Education Authority (HEA) and the Ireland's EU Structural Funds Programmes department of Jobs, Enterprise and Innovation, the Fulbright Ireland Student Award in Science, granted by the Board of the Fulbright Commission, and the Pierce Malone Scholarship in Engineering, from the National University of Ireland, to FEG. The European Research Council (ERC) under Grant No. 258992 (BONEMECHBIO) and the European Regional Development Fund through the Science Foundation Ireland (SFI) Investigators Programme to LMM. This work was additionally funded by the National Institute of Health (NIH) under Grant No. AI109499 to TCM.

List of Symbols and Abbreviations

MSC	mesenchymal stem cell
Mesensphere	mesenchymal stem cell spheroid
PBS	Phosphate Buffered Saline
—N	N-cadherin siRNA treated MSCs
—OB	OB-cadherin siRNA treated MSCs
Scram	scrambled siRNA treated MSCs
siRNA	small interfering RNA
SLS	Standard Linear Solid
$\boldsymbol{u(t)}$	creep displacement at time t
$\boldsymbol{D_0}$	initial mesensphere diameter
$\boldsymbol{\sigma_0}$	nominal stress
$\boldsymbol{E_0}$	instantaneous Young's modulus
$\boldsymbol{E_\infty}$	long term Young's modulus
μ	apparent viscosity

References

Baraniak P, McDevitt T, 2012 Scaffold-free culture of mesenchymal stem cell spheroids in suspension preserves multilineage potential. Cell Tissue Res. 347 (3), 701–711. [PubMed: 21833761]

Chopra A, Tabdanov E, Patel H, Janmey PA, Kresh JY, 2011 Cardiac myocyte remodeling mediated by N-cadherin-dependent mechanosensing. Am. J. Physiol. -Heart Circul. Physiol 300 (4), H1252.

Cook MM, Futrega K, Osiecki M, Kabiri M, Kul B, Rice A, Atkinson K, Brooke G, Doran M, 2012 Micromarrows—three-dimensional coculture of hematopoietic stem cells and mesenchymal stromal cells. Tissue Eng. Part C: Methods 18 (5), 319–328. [PubMed: 22082070]

Darling EM, Topel M, Zauscher S, Vail TP, Guilak F, 2008 Viscoelastic properties of human mesenchymally-derived stem cells and primary osteoblasts, chondrocytes, and adipocytes. J. Biomech 41 (2), 454–464. [PubMed: 17825308]

Engler AJ, Griffin MA, Sen S, Bönnemann CG, Sweeney HL, Discher DE, 2004 Myotubes differentiate optimally on substrates with tissue-like stiffness pathological implications for soft or stiff microenvironments. J. Cell Biol. 166 (6), 877–887. [PubMed: 15364962]

Engler AJ, Sen S, Sweeney HL, Discher DE, 2006 Matrix elasticity directs stem cell lineage specification. Cell 126 (4), 677–689. [PubMed: 16923388]

Freeman FE, Haugh M, McNamara L, 2013 Investigation of the optimal timing for chondrogenic priming of MSCs to enhance osteogenic differentiation in vitro as a bone tissue engineering strategy. J. Tissue Eng. Regenerative Med

Freeman FE, Haugh MG, McNamara L, 2015 An in vitro bone tissue regeneration strategy combining chondrogenic and vascular priming enhances the mineralisation potential of MSCs in vitro whilst also allowing for vessel formation. Tissue Eng. Part A 21 (7–8), 1320–1332. [PubMed: 25588588]

Freeman FE, Stevens H, Owens P, Guldberg R, McNamara L, 2016 Osteogenic differentiation of MSCs by mimicking the cellular niche of the endochondral template. Tissue Eng. Part A 22 (19–20).

Fujita H, Yamamoto M, Ogino T, Kobuchi H, Ohmoto N, Aoyama E, Oka T, Nakanishi T, Inoue K, Sasaki J, 2014 Necrotic and apoptotic cells serve as nuclei for calcification on osteoblastic differentiation of human mesenchymal stem cells in vitro. Cell Biochem. Funct 32 (1), 77–86. [PubMed: 23657822]

Ganz A, Lambert M, Saez A, Silberzan P, Buguin A, Mège RM, Ladoux B, 2006 Traction forces exerted through N-cadherin contacts. Biol. Cell 98 (12), 721–730. [PubMed: 16895521]

Gilbert SF, 2000 Osteogenesis: the development of bones.

Guntur AR, Rosen CJ, Naski MC, 2012 N-cadherin adherens junctions mediate osteogenesis through PI3K signaling. Bone 50 (1), 54–62. [PubMed: 21964322]

Haider MA, Guilak F, 2002 An axisymmetric boundary integral model for assessing elastic cell properties in the micropipette aspiration contact problem. J. Biomech. Eng 124 (5), 586–595. [PubMed: 12405602]

Hall BK, Miyake T, 2000 All for one and one for all: condensations and the initiation of skeletal development. BioEssays 22 (2), 138–147. [PubMed: 10655033]

Hong S, Troyanovsky RB, Troyanovsky SM, 2013 Binding to F-actin guides cadherin cluster assembly, stability, and movement. J. Cell Biol. 201 (1), 131–143. [PubMed: 23547031]

Hsu S-H, Huang G-S, 2013 Substrate-dependent Wnt signaling in MSC differentiation within biomaterial-derived 3D spheroids. Biomaterials 34 (20), 4725–4738. [PubMed: 23562051]

Huebsch N, Arany PR, Mao AS, Shvartsman D, Ali OA, Bencherif SA, Rivera-Feliciano J, Mooney DJ, 2010 Harnessing traction-mediated manipulation of the cell/matrix interface to control stem-cell fate. Nat. Mater 9 (6), 518–526. [PubMed: 20418863]

Huveneers S, Oldenburg J, Spanjaard E, van der Krogt G, Grigoriev I, Akhmanova A, Rehmann H, de Rooij J, 2012 Vinculin associates with endothelial VE-cadherin junctions to control force-dependent remodeling. J. Cell Biol. 196 (5), 641–652. [PubMed: 22391038]

Kabiri M, Kul B, Lott WB, Futrega K, Ghanavi P, Upton Z, Doran MR, 2012 3D mesenchymal stem/stromal cell osteogenesis and autocrine signalling. Biochem. Biophys. Res. Commun 419 (2), 142–147. [PubMed: 22266317]

Kanczler J, Oreffo R, 2008 Osteogenesis and angiogenesis: the potential for engineering bone. Eur. Cell Mater. 15 (2), 100–114. [PubMed: 18454418]

Karaplis AC, 2002 Embryonic development of bone and the molecular regulation of intramembranous and endochondral bone formation. Prin. Bone Biol. 1, 33–58.

Kawaguchi J, Kii I, Sugiyama Y, Takeshita S, Kudo A, 2001 The transition of cadherin expression in osteoblast differentiation from mesenchymal cells: consistent expression of cadherin-11 in osteoblast lineage. J. Bone Miner. Res 16 (2), 260–269. [PubMed: 11204426]

Kinney MA, Saeed R, McDevitt TC, 2012 Systematic analysis of embryonic stem cell differentiation in hydrodynamic environments with controlled embryoid body size. Integr. Biol 4 (6), 641–650.

Kinney MA, Saeed R, McDevitt TC, 2014 Mesenchymal morphogenesis of embryonic stem cells dynamically modulates the biophysical microtissue niche. Sci. Rep 4.

Ladoux B, Anon E, Lambert M, Rabodzey A, Hersen P, Buguin A, Silberzan P, Mège R-M, 2010 Strength dependence of cadherin-mediated adhesions. Biophys. J 98 (4), 534–542. [PubMed: 20159149]

Lee C-H, Hong C-H, Chen Y-T, Chen Y-C, Shen M-R, 2012 TGF-beta1 increases cell rigidity by enhancing expression of smooth muscle actin: keloid-derived fibroblasts as a model for cellular mechanics. J. Dermatol. Sci 67 (3), 173–180. [PubMed: 22771320]

Liu Z, Tan JL, Cohen DM, Yang MT, Sniadecki NJ, Ruiz SA, Nelson CM, Chen CS, 2010 Mechanical tugging force regulates the size of cell–cell junctions. Proc. Natl. Acad. Sci 107 (22), 9944–9949. [PubMed: 20463286]

Luu HH, Song WX, Luo X, Manning D, Luo J, Deng ZL, Sharff KA, Montag AG, Haydon RC, He TC, 2007 Distinct roles of bone morphogenetic proteins in osteogenic differentiation of mesenchymal stem cells. J. Orthop. Res 25 (5), 665–677. [PubMed: 17290432]

Mani SA, Guo W, Liao M-J, Eaton EN, Ayyanan A, Zhou AY, Brooks M, Reinhard F, Zhang CC, Shipitsin M, 2008 The epithelial-mesenchymal transition generates cells with properties of stem cells. Cell 133 (4), 704–715. [PubMed: 18485877]

Maruthamuthu V, Sabass B, Schwarz US, Gardel ML, 2011 Cell-ECM traction force modulates endogenous tension at cell–cell contacts. Proc. Natl. Acad. Sci 108 (12), 4708–4713. [PubMed: 21383129]

McCloy RA, Rogers S, Caldon CE, Lorca T, Castro A, Burgess A, 2014 Partial inhibition of Cdk1 in G2 phase overrides the SAC and decouples mitotic events. Cell Cycle 13 (9), 1400–1412. [PubMed: 24626186]

Mullen CA, Haugh MG, Schaffler MB, Majeska RJ, McNamara LM, 2013 Osteocyte differentiation is regulated by extracellular matrix stiffness and intercellular separation. J. Mech. Behav. Biomed. Mater 28, 183–194. [PubMed: 23994943]

Nelson WJ, Nusse R, 2004 Convergence of Wnt, ß-Catenin, and Cadherin pathways. Science 303 (5663), 1483–1487. [PubMed: 15001769]

Oberlender SA, Tuan RS, 1994 Spatiotemporal profile of N-cadherin expression in the developing limb mesenchyme. Cell Commun. Adhes 2 (6), 521–537.

Overduin M, Harvey TS, Bagby S, Tong KI, Yau P, Takeichi M, Ikura M, 1995 Solution structure of the epithelial cadherin domain responsible for selective cell adhesion. Science (New York, NY) 267 (5196), 386–389.

Pittet P, Lee K, Kulik AJ, Meister J-J, Hinz B, 2008 Fibrogenic fibroblasts increase intercellular adhesion strength by reinforcing individual OB-cadherin bonds. J. Cell Sci. 121 (6), 877–886. [PubMed: 18303045]

Reynolds N, McGarry J, 2015 Single cell active force generation under dynamic loading–Part II: active modelling insights. Acta Biomater. 27, 251–263. [PubMed: 26360595]

Ronan W, Deshpande VS, McMeeking RM, McGarry JP, 2012 Numerical investigation of the active role of the actin cytoskeleton in the compression resistance of cells. J. Mech. Behav. Biomed. Mater 14, 143–157. [PubMed: 23026692]

Ronan W, McMeeking RM, Chen CS, McGarry JP, Deshpande VS, 2015 Cooperative contractility: the role of stress fibres in the regulation of cell-cell junctions. J. Biomech 48 (3), 520–528. [PubMed: 25553672]

Sachlos E, Auguste DT, 2008 Embryoid body morphology influences diffusive transport of inductive biochemicals: a strategy for stem cell differentiation. Biomaterials 29 (34), 4471–4480. [PubMed: 18793799]

Shapiro L, Fannon AM, Kwong PD, Thompson A, Lehmann MS, Grubel G, Legrand J-F, Als-Nielsen J, Colman DR, Hendrickson WA, 1995 Structural basis of cell-cell adhesion by cadherins. Nature 374 (6520), 327–337. [PubMed: 7885471]

Shin CS, Lecanda F, Sheikh S, Weitzmann L, Cheng S-L, Civitelli R, 2000 Relative abundance of different cadherins defines differentiation of mesenchymal precursors into osteogenic, myogenic, or adipogenic pathways. J. Cell. Biochem 78 (4), 566–577. [PubMed: 10861854]

Simmons CA, Matlis S, Thornton AJ, Chen S, Wang C-Y, Mooney DJ, 2003 Cyclic strain enhances matrix mineralization by adult human mesenchymal stem cells via the extracellular signal-regulated kinase (ERK1/2) signaling pathway. J. Biomech 36 (8), 1087–1096. [PubMed: 12831733]

Stains JP, Civitelli R, 2005 Cell-to-cell interactions in bone. Biochem. Biophys. Res. Commun 328 (3), 721–727. [PubMed: 15694406]

Tan S, Fang JY, Yang Z, Nimni ME, Han B, 2014 The synergetic effect of hydrogel stiffness and growth factor on osteogenic differentiation. Biomaterials 35 (20), 5294–5306. [PubMed: 24703716]

Thompson T, Owens P, Wilson D, 1989 Intramembranous osteogenesis and angiogenesis in the chick embryo. J. Anat 166, 55. [PubMed: 2482839]

Titushkin I, Cho M, 2007 Modulation of cellular mechanics during osteogenic differentiation of human mesenchymal stem cells. Biophys. J 93 (10), 3693–3702. [PubMed: 17675345]

Wang L, Fan H, Zhang Z-Y, Lou A-J, Pei G-X, Jiang S, Mu T-W, Qin J-J, Chen S-Y, Jin D, 2010 Osteogenesis and angiogenesis of tissue-engineered bone constructed by prevascularized β-tricalcium phosphate scaffold and mesenchymal stem cells. Biomaterials 31 (36), 9452–9461. [PubMed: 20869769]

Wang W, Itaka K, Ohba S, Nishiyama N, Chung U-I, Yamasaki Y, Kataoka K, 2009 3D spheroid culture system on micropatterned substrates for improved differentiation efficiency of multipotent mesenchymal stem cells. Biomaterials 30 (14), 2705–2715. [PubMed: 19215979]

Watt FM, Hogan BLM, 2000 Out of Eden: stem cells and their niches. Science 287 (5457), 1427–1430. [PubMed: 10688781]

Weafer P, Reynolds N, Jarvis S, McGarry J, 2015 Single cell active force generation under dynamic loading–Part I: AFM experiments. Acta Biomater. 27, 236–250. [PubMed: 26360596]

Yin T, Li L, 2006 The stem cell niches in bone. J. Clin. Invest 116 (5), 1195–1201. [PubMed: 16670760]

Yonemura S, Wada Y, Watanabe T, Nagafuchi A, Shibata M, 2010 A-Catenin as a tension transducer that induces adherens junction development. Nat. Cell Biol. 12 (6), 533–542. [PubMed: 20453849]

Zimmermann JA, McDevitt TC, 2014 Pre-conditioning mesenchymal stromal cell spheroids for immunomodulatory paracrine factor secretion. Cytotherapy 16 (3), 331–345. [PubMed: 24219905]

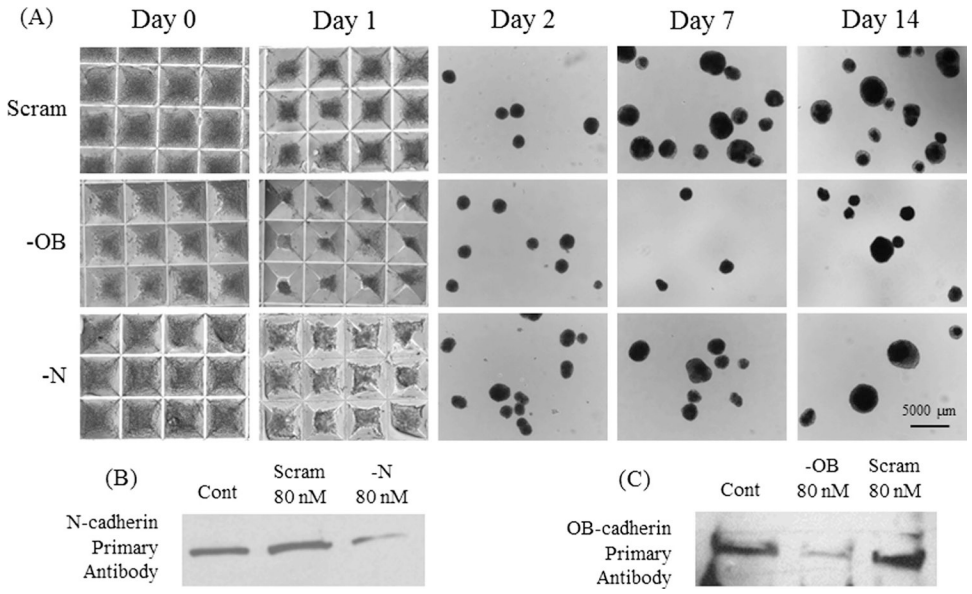

Fig. 1.

(A) Bright field images of mesensphere formation and at days 1, 2, 7 and 14. (B) Western Blot of N-cadherin siRNA (80 or 160 nM concentrations), scrambled siRNA at 80 nM concentration and untreated, control MSCs. (C) Western Blot of OB-cadherin siRNA (80 concentration), scrambled siRNA at 80 nM concentration and untreated, control MSCs. Groups: Cont: untreated control, Scram: scrambled siRNA, —N: N-cadherin siRNA, —OB: OB-cadherin siRNA.

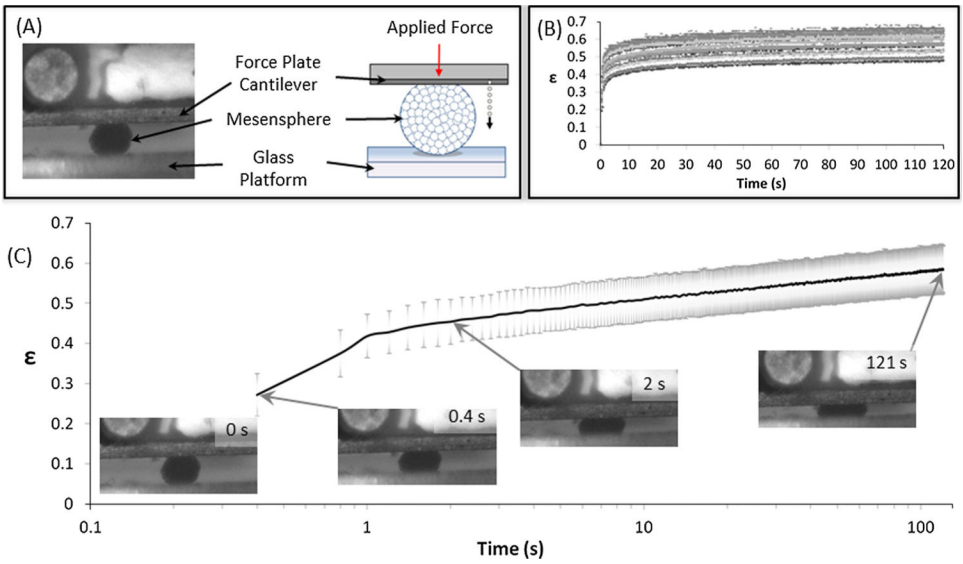

Fig. 2.

(A) Schematic of testing equipment including cantilever for force application (red arrow) and measurement, mesensphere and glass prism. Dotted arrow indicates motion tracking of cantilever displacement during compression of mesensphere. The mesensphere is placed on a glass prism and then a constant force is applied for the duration of the test. (B) Nominal creep strain (ε) calculated as tip displacement normalised to initial mesensphere height. Data from testing of $n = 19$ samples of day 2 Scrambled siRNA treated mesenspheres. (C) Nominal creep strain (ε) for day 2 Scrambled siRNA treated mesenspheres. The grey borders denote standard deviation of the data. Inset are representative Brightfield images showing the initial compression of the mesensphere by the cantilever at 0, 0.4, 2 s and the mesensphere in compression at the end of the test (121 s). (For interpretation of the references to colour in this figure legend, the reader is referred to the web version of this article.)

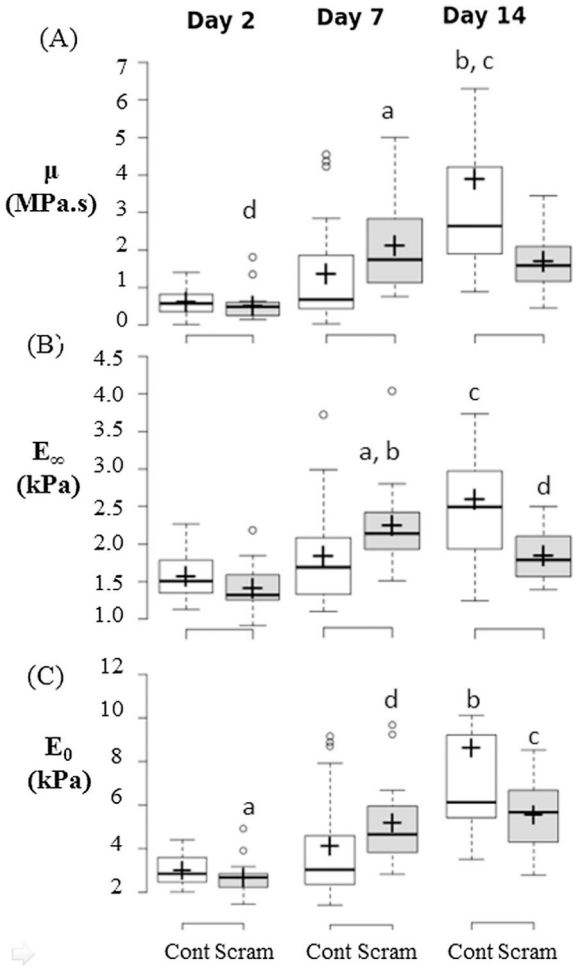

Fig. 3.

Scrambled siRNA treatment causes decrease in mesensphere viscosity (μ), long term Young's modulus (E_∞) and instantaneous Young's modulus (E_0). Box Plots of (A) Viscosity (μ), (B) Long Term Young's Modulus (E_∞), and (C) instantaneous Young's modulus (E_0) for untreated cells (Cont) and scrambled siRNA treated cells (Scram). Significance is declared at $p < 0.05$. For (A) a $p = 0.006$ vs. day 7 Cont, b: $p = 0.001$ vs. day 14 Scram, c: $p < 0.001$ vs. days 2 & 7 Cont, d: $p < 0.001$ vs. days 7 & 14 Scram. (B) a $p < 0.006$ vs. day 7 Cont, b $p < 0.001$ vs. days 2 Scram, c $p < 0.001$ vs. days 2 & 7 Cont & day 14 Scram, d $p = 0.001$ vs. days 2 & 7 Scram. (C) a: $p < 0.001$ vs. days 7 & 14 Scram, b: $p < 0.001$ vs. days 2 & 7 Cont, c: $p < 0.016$ vs. day 7 Cont.

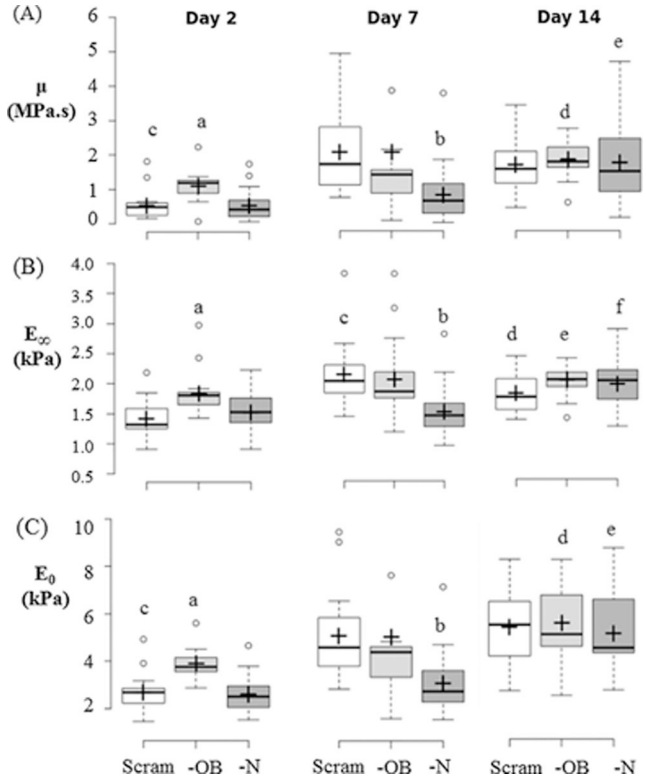

Fig. 4.

—OB mesensphere viscosity (μ), instantaneous Young's modulus (E_0) and long term Young's modulus (E_∞) are higher than Scram and —N at day 2. Box-plots of (A) μ, (B) E_∞, and (C) E_0 comparing between treatment groups during each time point or comparing between time points within each group for day 2, day 7, and day 14. Significance is declared at $p < 0.05$. (A) a: $p < 0.001$ vs day 2 Scram & —N, b: $p < 0.02$ vs. day 7 Scram & —OB, c: $p < 0.001$ vs. days 7 & 14 Scram, d: $p = 0.025$ vs. day 2 & 7 —OB, e: $p < 0.005$ vs. days 2 & 7 —N. (B) a: $p < 0.009$ vs. day 2 Scram & —N, b: $p < 0.002$ vs day 7 Scram & —OB, c: $p < 0.001$ vs days 2 Scram, d: $p = 0.04$ vs day 2 & 7 Scram, e: $p = 0.037$ vs day 2 —OB, day 14 SC, f: $p < 0.003$ vs days 2 & 7 —N. (C) a: $p < 0.001$ vs day 2 Scram & —N, b: $p < 0.009$ vs day 7 Scram & —OB, c: $p < 0.001$ vs days 7 & 14 Scram, d: $p < 0.007$ vs days 2 & 7 —OB, e: $p < 0.001$ vs days 2 & 7 —N. Groups: Scram: scrambled siRNA, —OB: OB-cadherin siRNA, —N: N-cadherin siRNA.

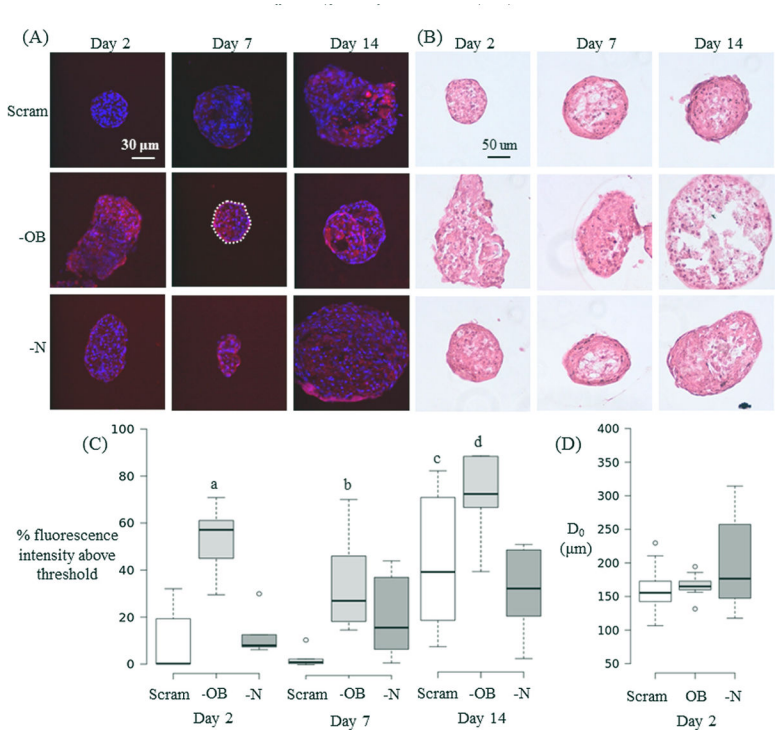

Fig. 5.

(A) Immunofluorescent images of mesenspheres at day 2, 7 and 14. The nucleus (blue) is stained with DAPI and the cytoskeleton (red) is stained with TRITC Phalloidin. The white dashed line in the central panel encloses the mesensphere area analysed for fluorescence intensity in that image. (B) H&E staining of mesenspheres at day 2, 7 and 14. (C) Boxplots of Day 2 cytoskeletal fluorescence showing % intensity above the threshold value. $n = 6$ samples for each group and time point. (D) Horizontal diameter of mesenspheres at day 2 measured before mechanical testing. Groups: scrambled siRNA (Scram), OB-cadherin siRNA (—OB), N-cadherin siRNA (—N). Kruskal-Wallis non-parametric tests were performed and significance is declared at $p < 0.05$. For (C) $a < 0.002$ vs. day 2 (Scram, —N). $b = 0.003$ vs. day 7 Scram. $c = 0.023$ vs. days 2 & 7 Scram. $d < 0.02$ vs. 7 (—OB) and day 14 (—N). (For interpretation of the references to colour in this figure legend, the reader is referred to the web version of this article.)

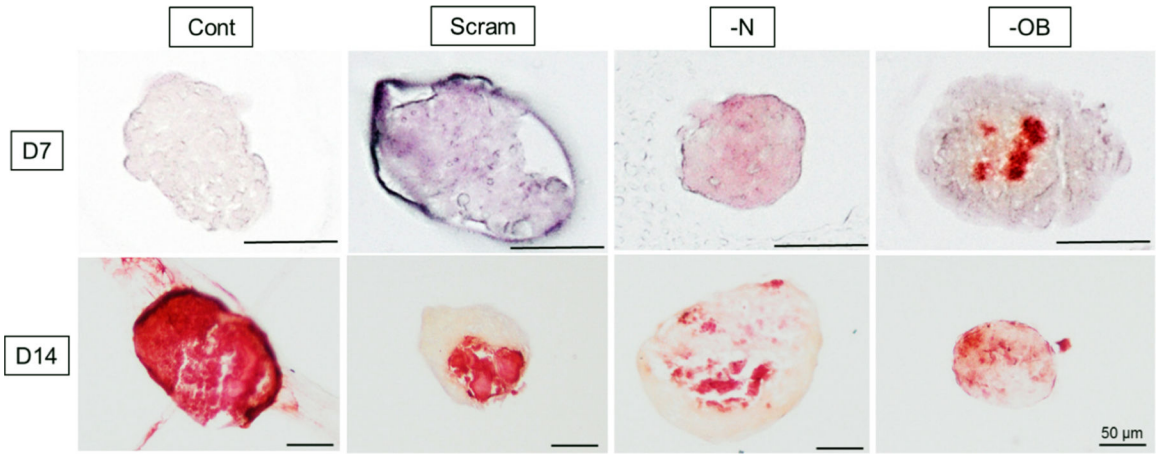

Fig. 6.

Alizarin Red staining of mesenspheres at day 7 and day 14 for all four treatment groups: Groups: Scram: scrambled siRNA, —OB: OB-cadherin siRNA, —N: N-cadherin siRNA. Scale bars represent 50 μm.

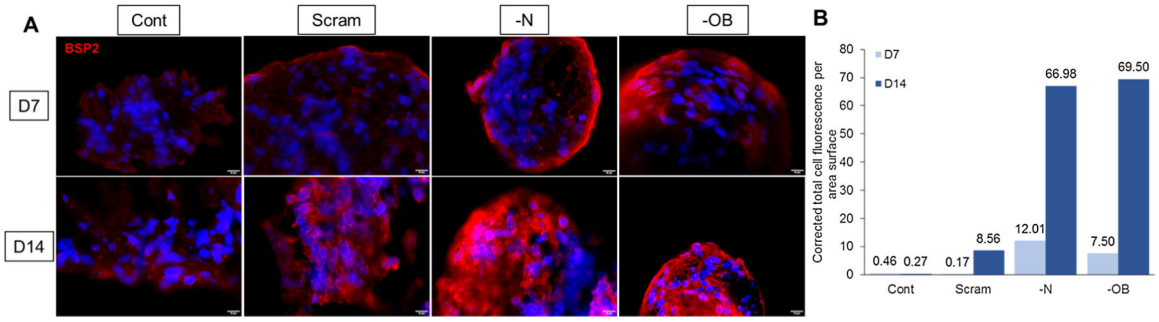

Fig. 7.

BMP2 immunofluorescent staining of mesenspheres at day 7 and day 14. Groups: Scram: scrambled siRNA, —OB: OB-cadherin siRNA, —N: N-cadherin siRNA. Scale bars represent 10 μm. The corrected total cell fluorescence per area surface was measured for each condition (B).

Table 1

Summary table of viscoelastic material constants for Osteogenic control (Control), scrambled siRNA (Scram), OB-cadherin siRNA (—OB), N-cadherin siRNA (—N) treatment groups at days 2, 7 and 14.

		Instantaneous Young's Modulus (E_0) (Pa)		Relaxed Young's Modulus (E_∞) (Pa)		Viscosity (μ) (Pa s)	
	Day	**Avg.**	**St. Dev.**	**Avg.**	**St. Dev.**	**Avg.**	**St. Dev.**
Cont	2	3060	664	1576	312	6.03E+05	3.29E+05
Scram		2690	789	1422	315	5.32E+05	4.12E+05
—OB		3910	576	1839	346	1.09E+06	4.17E+05
—N		2610	845	1518	364	5.22E+05	4.62E+05
Cont	7	3870	2300	1801	715	1.33E+06	1.48E+06
Scram		5130	1920	2198	556	2.04E+06	1.17E+06
—OB		5090	3730	2116	671	2.03E+06	2.52E+06
—N		3140	1380	1555	444	8.12E+05	8.59E+05
Cont	14	8640	8860	2552	851	3.76E+06	4.49E+06
Scram		5320	1750	1817	313	1.63E+06	7.99E+05
—OB		5790	1450	2046	257	1.80E+06	5.29E+05
—N		5300	1680	1978	417	1.69E+06	1.09E+06

Table 2

Pearsons Correlation Coefficient (r) and correlation significance (p) for the correlation between mesensphere diameter and viscosity (μ), Long term Young's Modulus (E_∞), and instantaneous Young's Modulus (E_0). Groups: Osteogenic control (Control), scrambled siRNA (Scram), OB-cadherin siRNA (—OB), N-cadherin siRNA (—N).

		Viscosity (μ)			Relaxed Young's Modulus (E_∞)			Relaxed Young's Modulus (E_0)		
		D2	D7	D14	D2	D7	D14	D2	D7	D14
Control	r	−0.517	0.125	−0.439	−0.297	0.035	−0.379	−0.323	0.104	−0.414
	p	0.023	0.609	0.060	0.217	0.888	0.109	0.178	0.671	0.078
Scram	r	−0.769	−0.209	−0.378	−0.846	−0.150	−0.466	−0.873	−0.300	−0.335
	P	0.001	0.404	0.111	0.001	0.553	0.044	0.001	0.227	0.161
—OB	r	−0.700	−0.210	−0.086	−0.539	−0.160	−0.034	−0.856	0.142	−0.072
	P	0.001	0.387	0.728	0.017	0.512	0.889	0.001	0.563	0.771
—N	r	0.271	0.109	−0.068	0.201	0.182	0.011	0.219	0.111	−0.152
	P	0.261	0.656	0.783	0.410	0.456	0.965	0.368	0.651	0.535